The cycle of baryons in Brightest Cluster Galaxies

Paolo Tozzi
INAF
Oss. Astrofisico di Arcetri

Galaxy Evolution and Environment - Arcetri, November 17, 2017

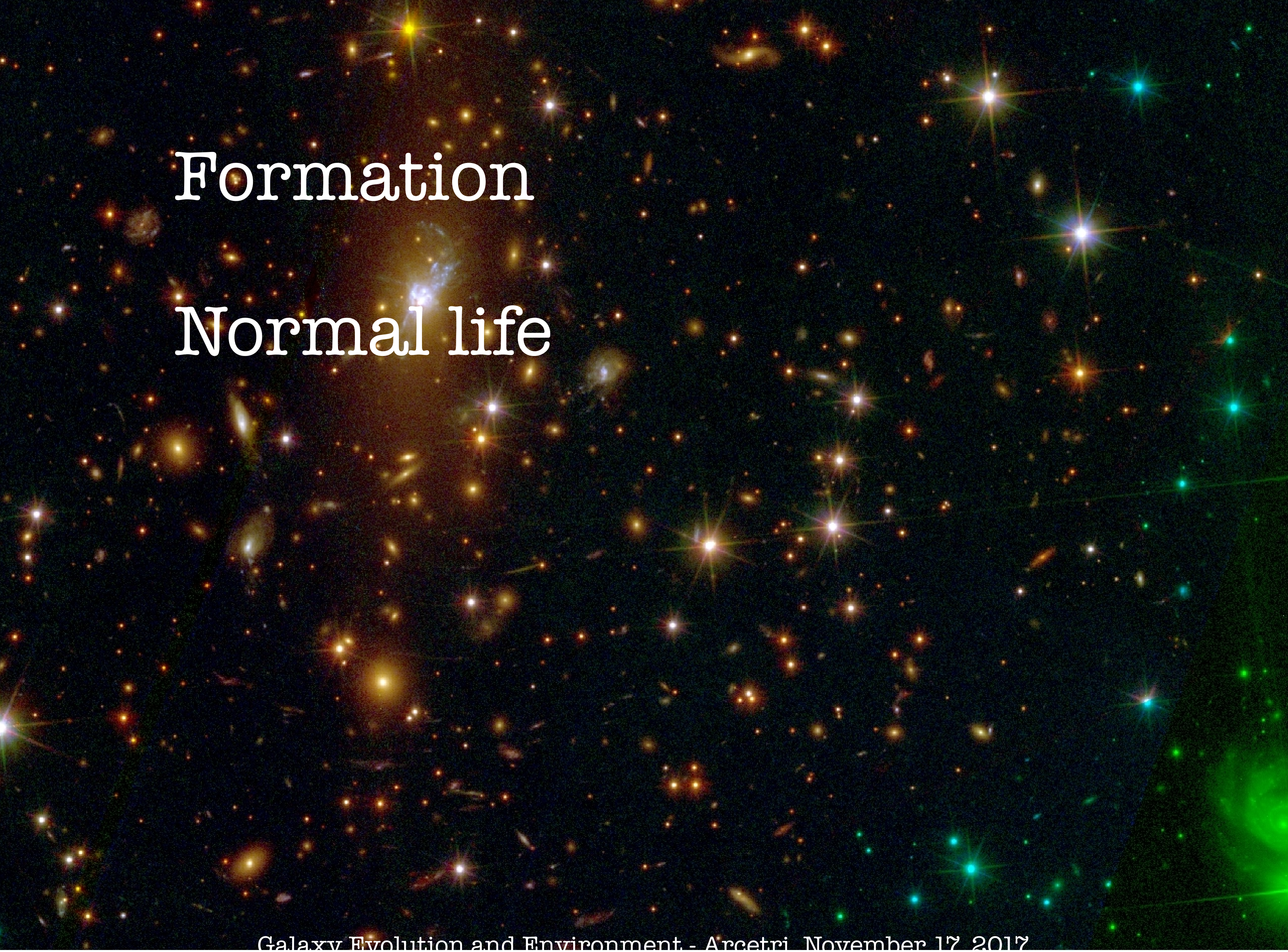
Formation
Normal life

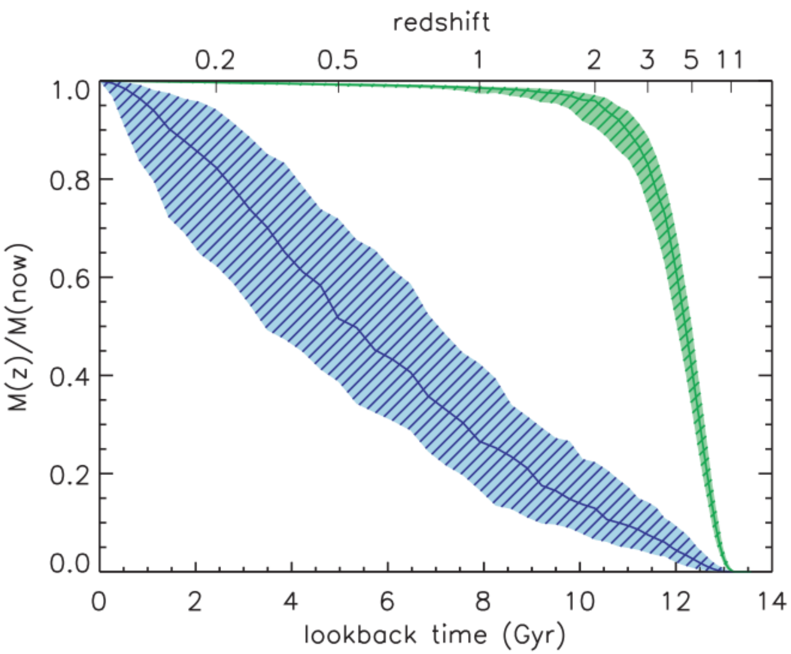

Figure 7. Assembly (blue) and formation (green) histories of our sample of BCGs selected at redshift 0 (as in Fig. 3). Thick lines show the median of the distributions, while the dashed regions show the 15th to 85th percentile range.

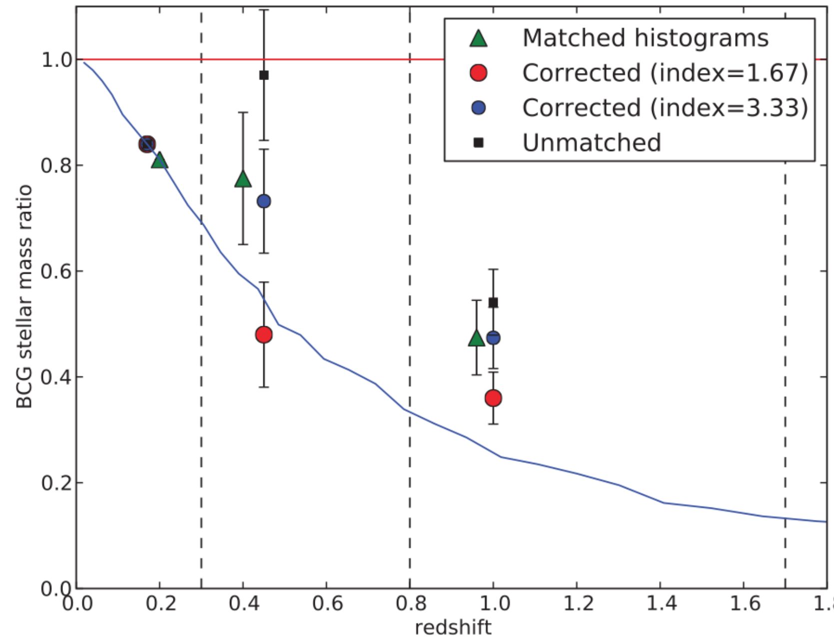

e **6.** The evolution in the median stellar mass of BCGs as a function shift. The green triangles take into account the correlation between mass and the stellar mass of its BCG by matching clusters according

De Lucia & Blaizot 2007

Lidman et al. 2012

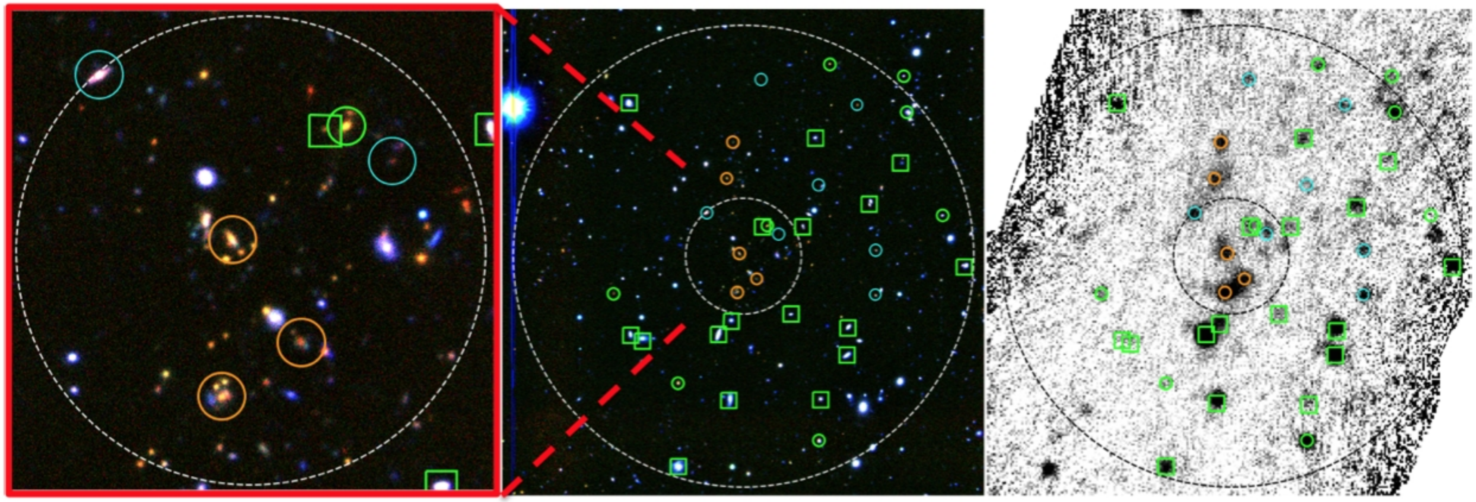

Figure 1. KsJI color composite of the central ~500 kpc (left) of the field of XDCP0044 (middle) and corresponding *Herschel*/PACS 100 μm map (right). Dashed circles have radii of 30″ and 2′ centered on the cluster X-ray center. The 5 spectroscopic members with FIR emission are shown in orange circles, cyan regions indicate the photometric candidates with FIR emission and green regions correspond to spectroscopic (circles) and visual/photo-z (squares) interlopers.

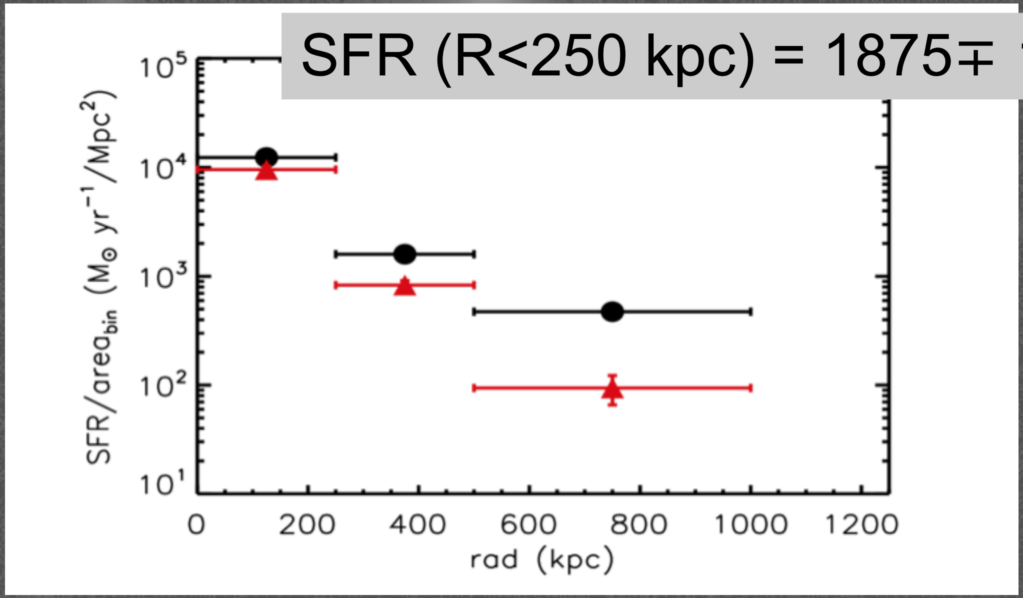

SFR (R<250 kpc) = 1875∓ 160 M/year

Santos et al. 2015

XMM0044 HST image

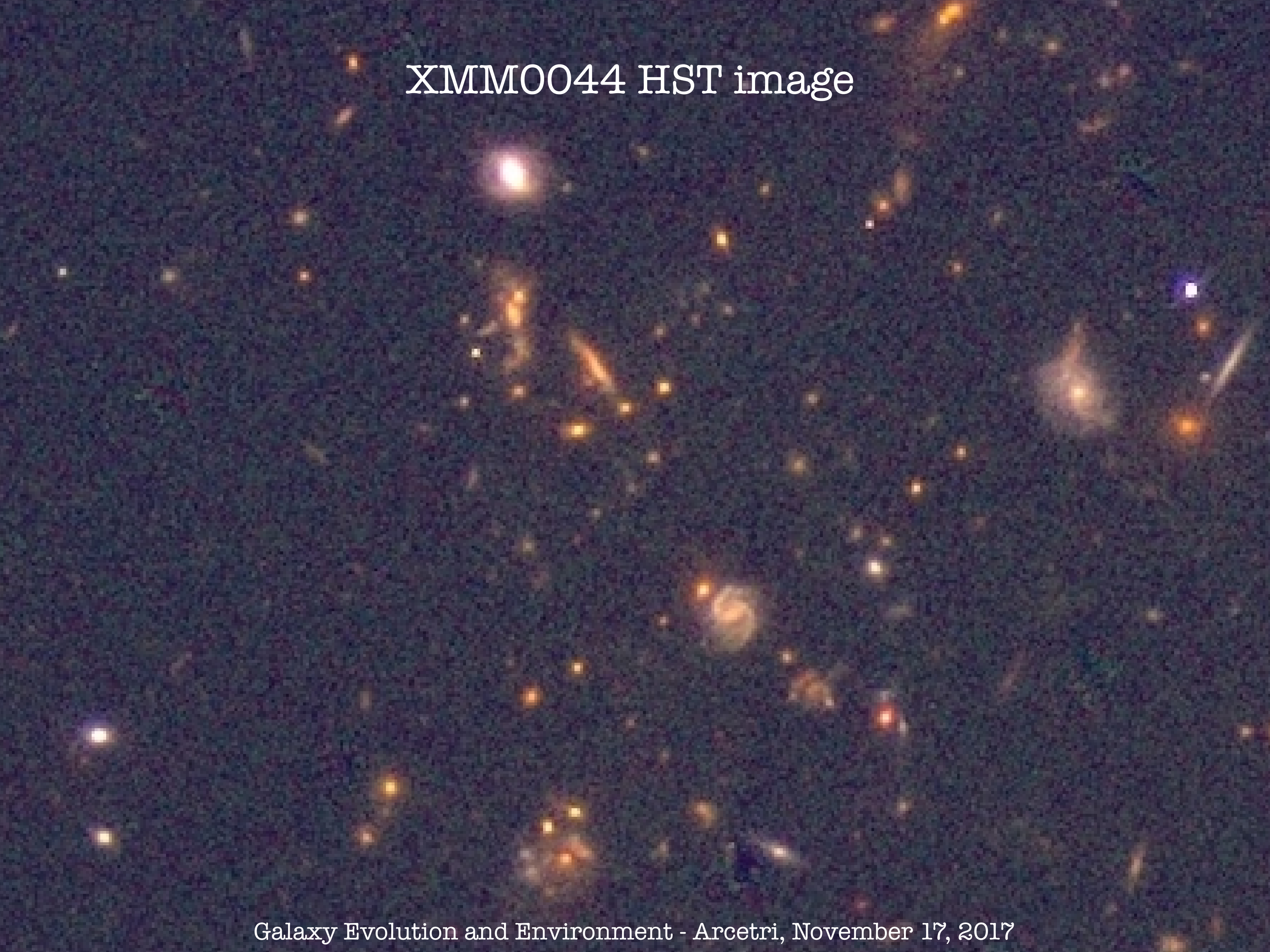

Chandra Deep Observation of XDCP J0044.0-2033

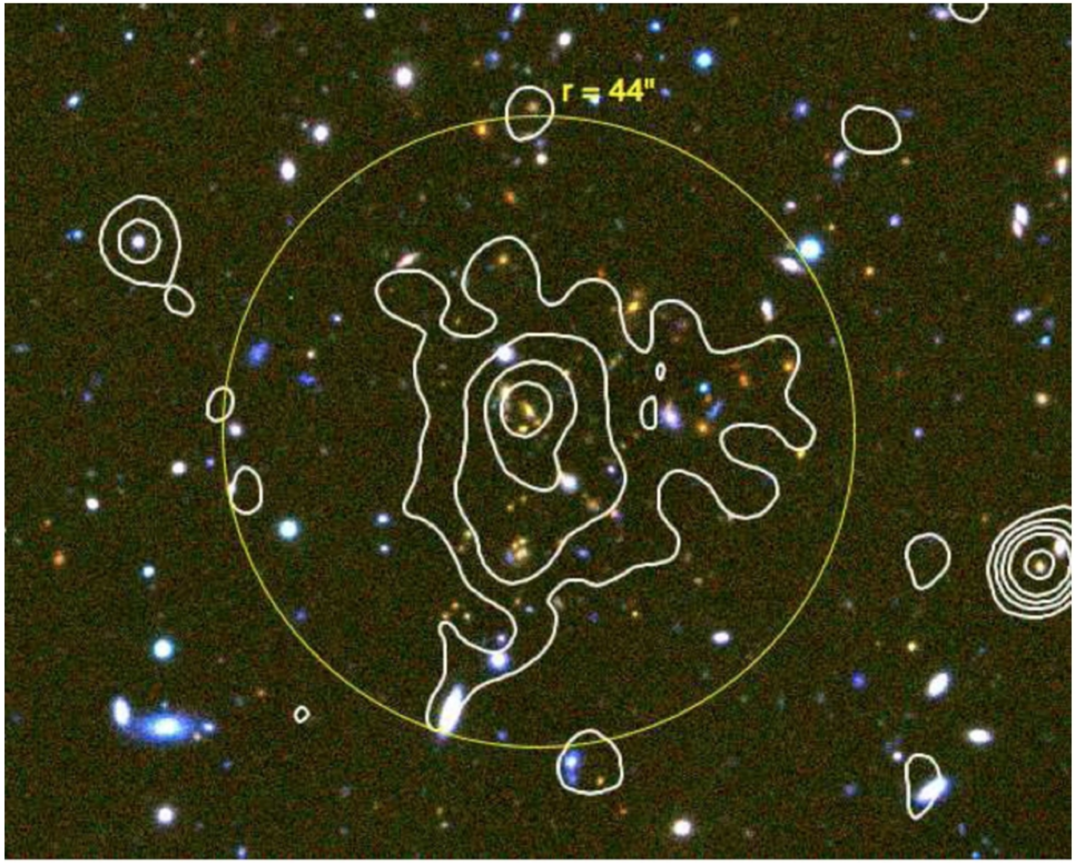

Figure 1. Optical *IJKs* color image of XDCP0044 with *Chandra* smoothed soft-band contours overlaid. Contours correspond to levels of 0.11, 0.3, 0.6 and 1.0 counts per pixel, to be compared with a background level of 3.5×10^{-2} counts per pixel in the original image (1 pixel = 0.″492). The image is obtained from Subaru/Suprime-Cam (*V* and *i* bands) and Hawk-I at VLT (*J* and *Ks* band) and has a size of $2.'5 \times 2'$. The solid circle has a radius of 44″ (corresponding to 375 kpc at $z = 1.58$), and shows the region used for the X-ray spectral analysis.

PT et al. 2015

Chandra Deep Observation of XDCP J0044.0-2033

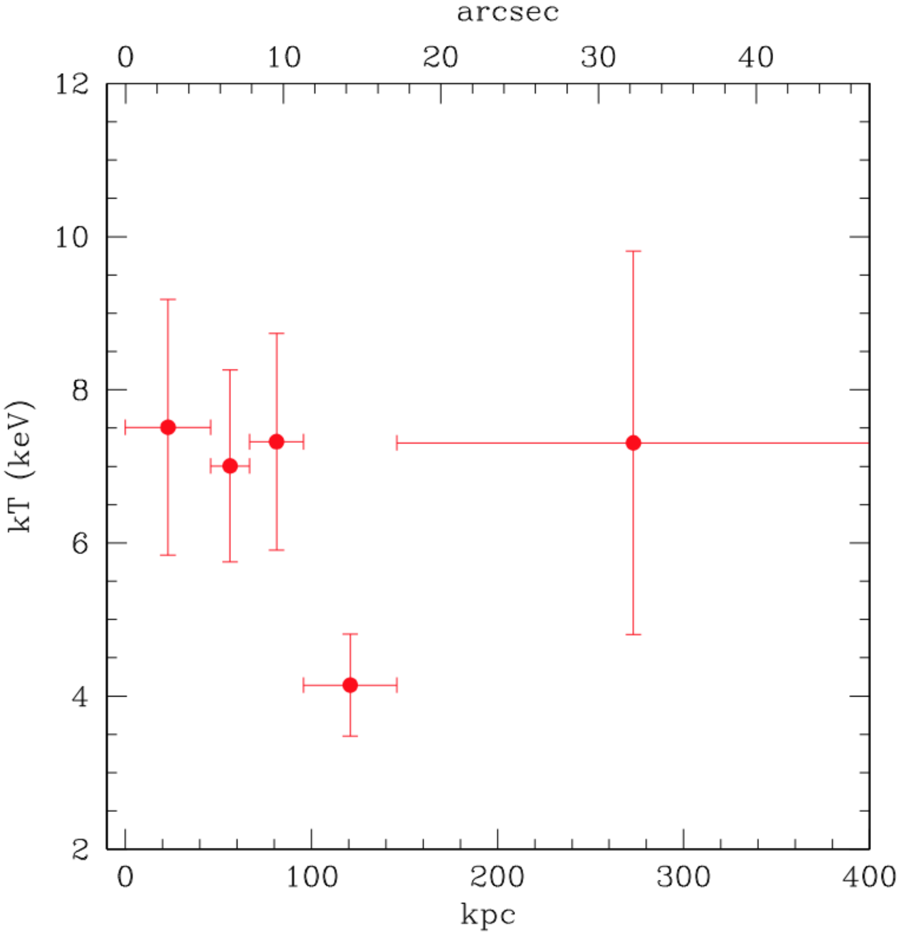

Figure 5. Projected temperature profile from the spatially resolved spectral analysis of XDCP0044. Each bin includes about 300 net counts in the 0.5–7 keV band.

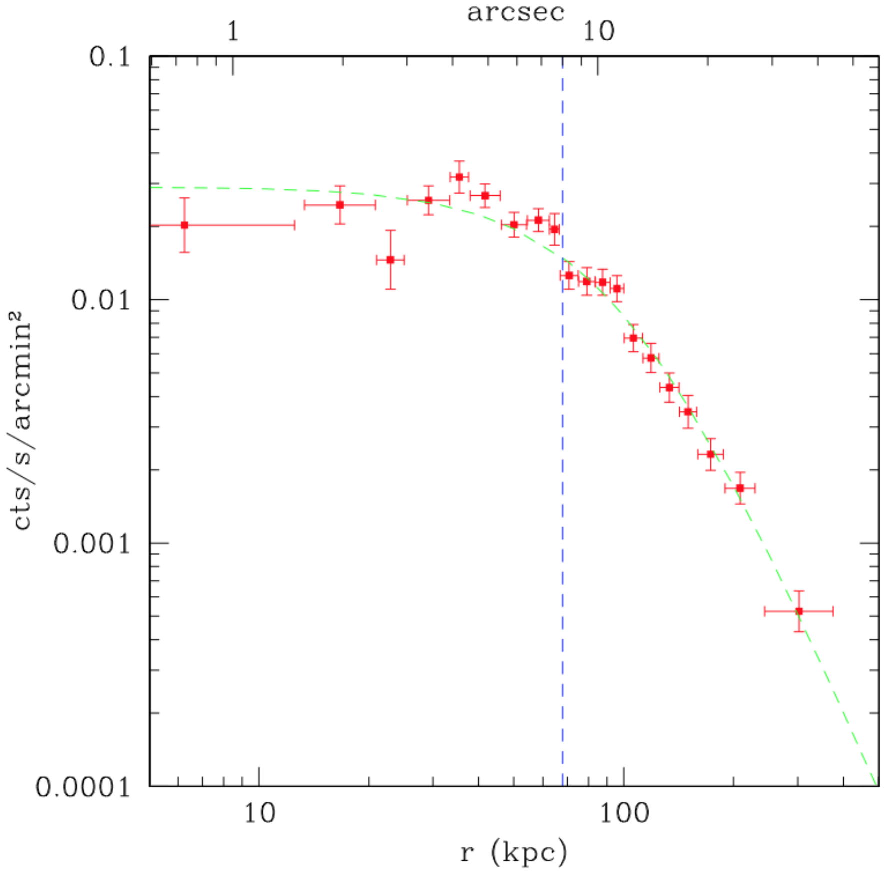

Figure 7. Background-subtracted surface brightness profile in the soft (0.5–2 keV) band (points) and best-fit β model (green dashed line) for XDCP0044. Error bars correspond to 1σ uncertainty. The vertical dashed line corresponds to the distance of the border of the northern clump from the X-ray centroid.

PT et al. 2015

Color image of XMM2235 from the combination of i, z (HST/ACS) and Ks (VLT/ISAAC) filters. Overlaid X-ray contours from Chandra (196 ks)

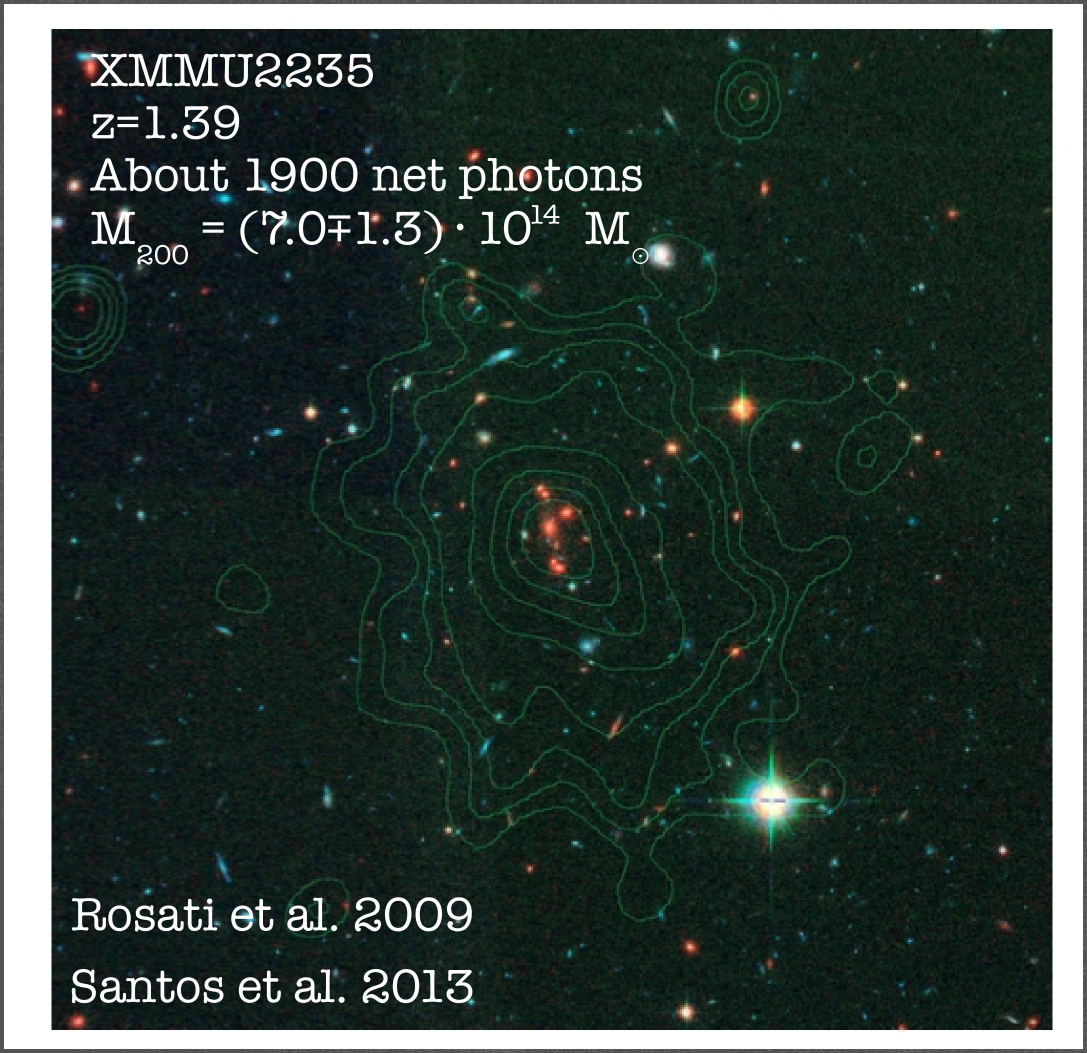

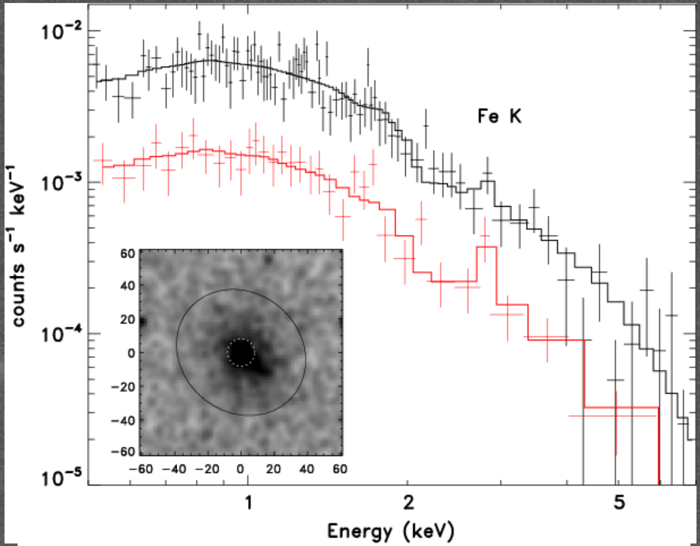

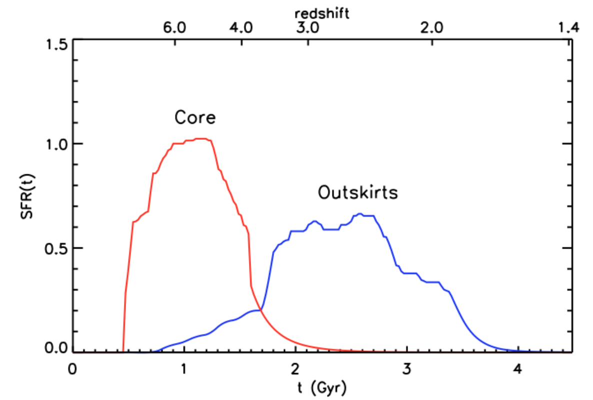

Fig. 5. Star formation histories (in arbitrary units) derived from the fit of the composite spectro-photometric data with BC03 τ-models for the sample of passive galaxies in the core and outskirts of XMM2235. The lower x-axis shows cosmic time; the upper x-axis marks the corresponding redshift.

The highest-z virialized (?) massive halo

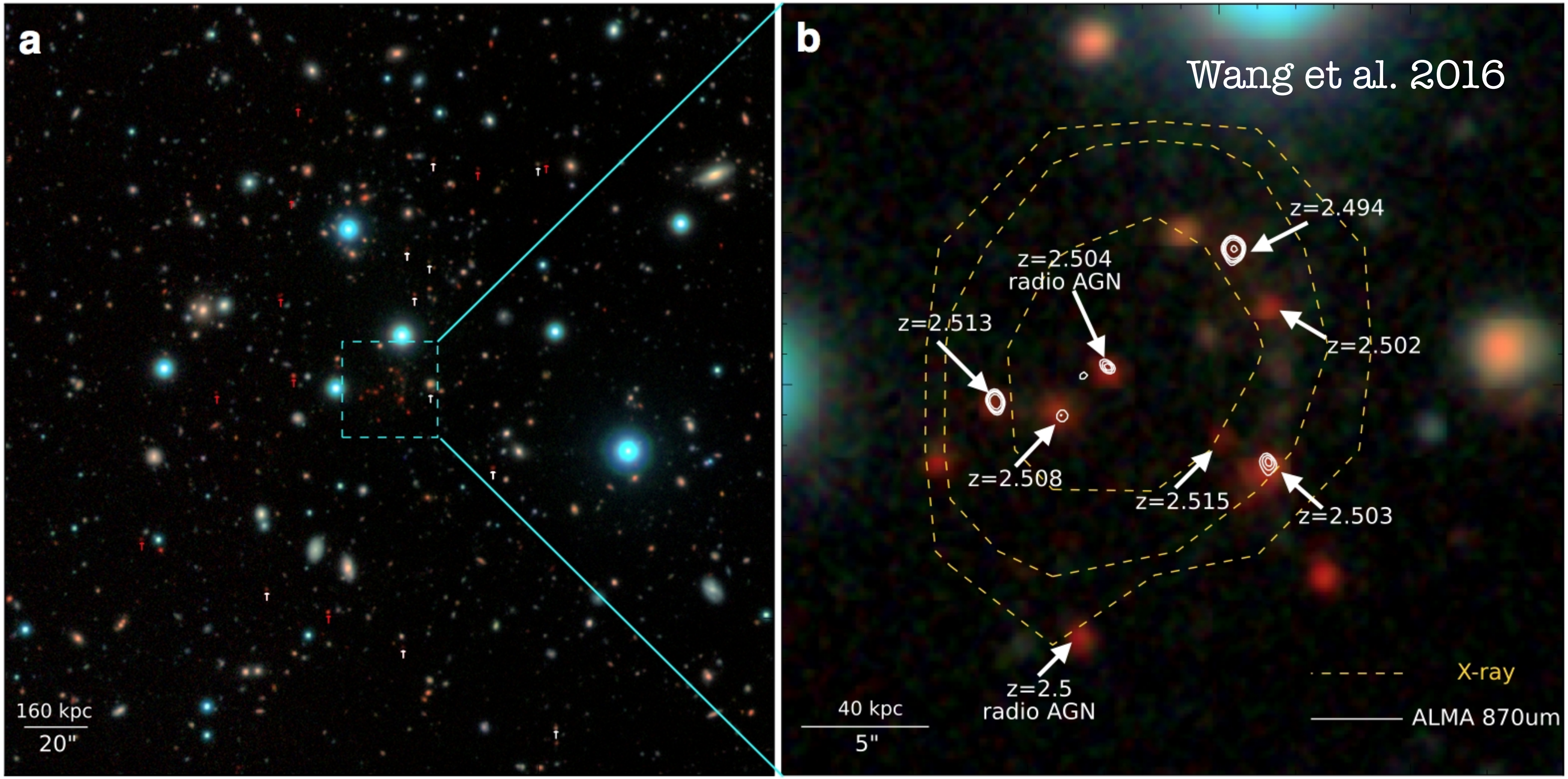

Figure 3. RGB composite color image of the region around the cluster core. The R, G and B channel correspond to the K_s, J and Y bands from the UltraVISTA survey, respectively. The left panel (**a**) corresponds to a $4' \times 4'$ region while the right panel (**b**) is an enlarged image of the central $30'' \times 30''$ region around the cluster core. Red arrows indicate distant red galaxies (DRGs) outside the core with $z_{phot} = 2.5 \pm 0.5$ while white arrows indicate spectroscopically confirmed members within 3σ of the peak of the redshift distribution ($z_{spec} = 2.506 \pm 0.018$), including 7 galaxies in the core (indicated in the right panel) and 10 galaxies in the outskirts. Extended X-ray emission (0.5-2 keV) and ALMA 870 μm continuum are overlaid, respectively, with yellow and white contours in the right panel. There are 11 DRGs (5 detected with ALMA at 870 μm) and 2 blue galaxies within the central $10''$ region, or 80 kpc at $z = 2.5$.

Radio selection of the most distant galaxy clusters

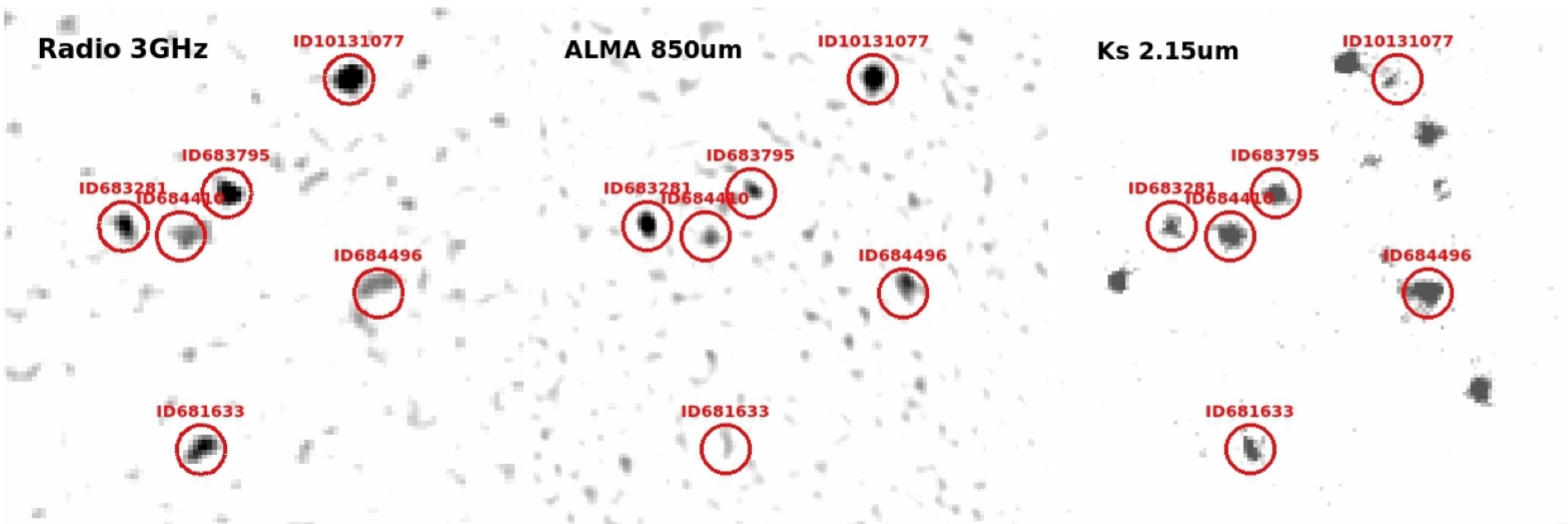

FIG. 1.— Maps of the W16 cluster region: VLA 3GHz (left), ALMA 850μm (center), Ks-band (right), all $\sim 0.7''$ resolution. Panels are $20''$. Small circles (1" radius) help localizing radio detected cluster members (all spectroscopically confirmed, see Table 1).

Daddi et al. 2017

Wide Field Survey X-ray Telescope – 5” FWHM on 1 sq deg

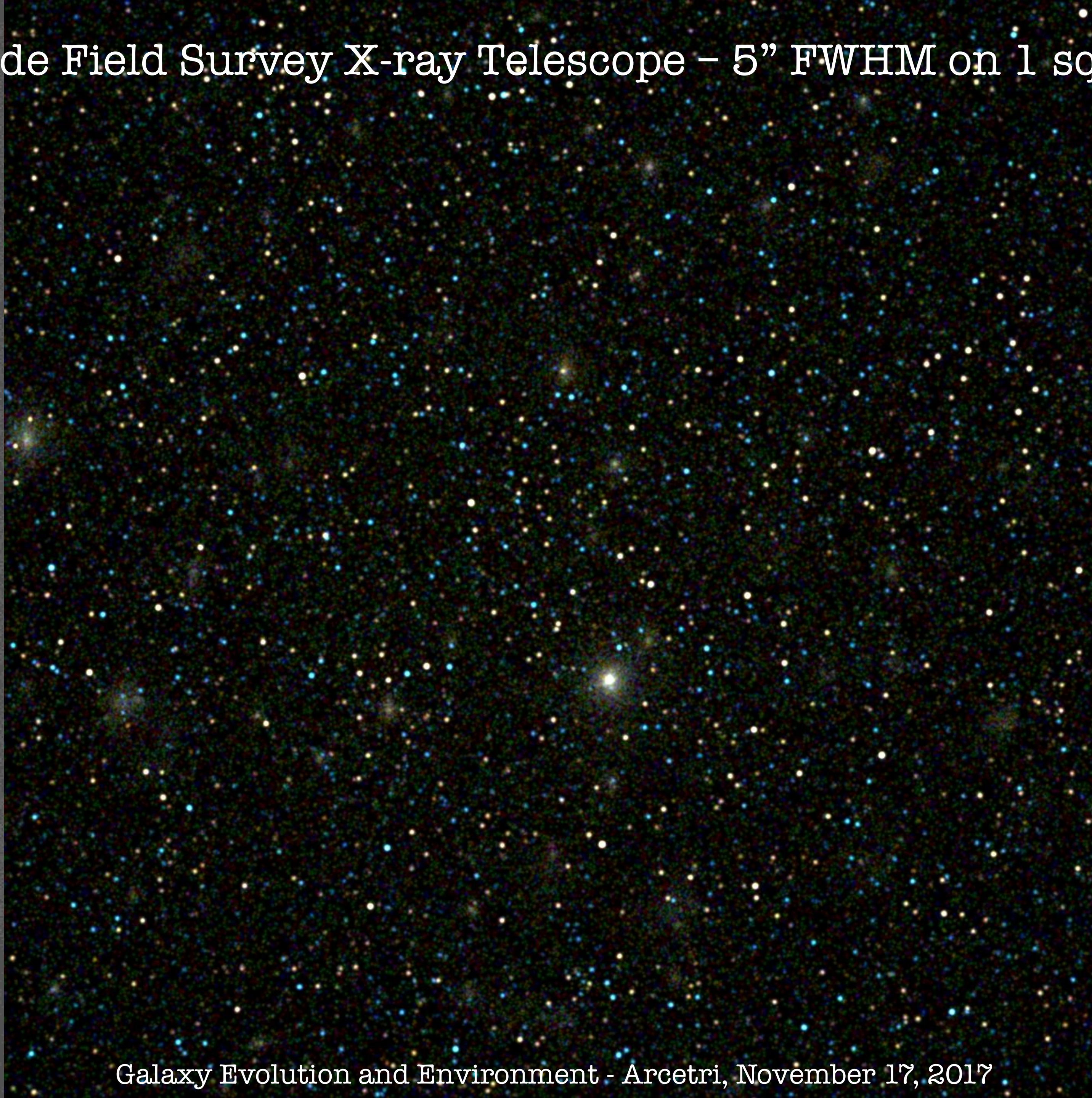

HST image, from the CLASH program (Postman et al. 2012)

JVLA CLASH follow-up, from Yu, PT et al. (2017) arXiv:1707.05336


MACS J1931.9-2634
Ehlert et al. 2011

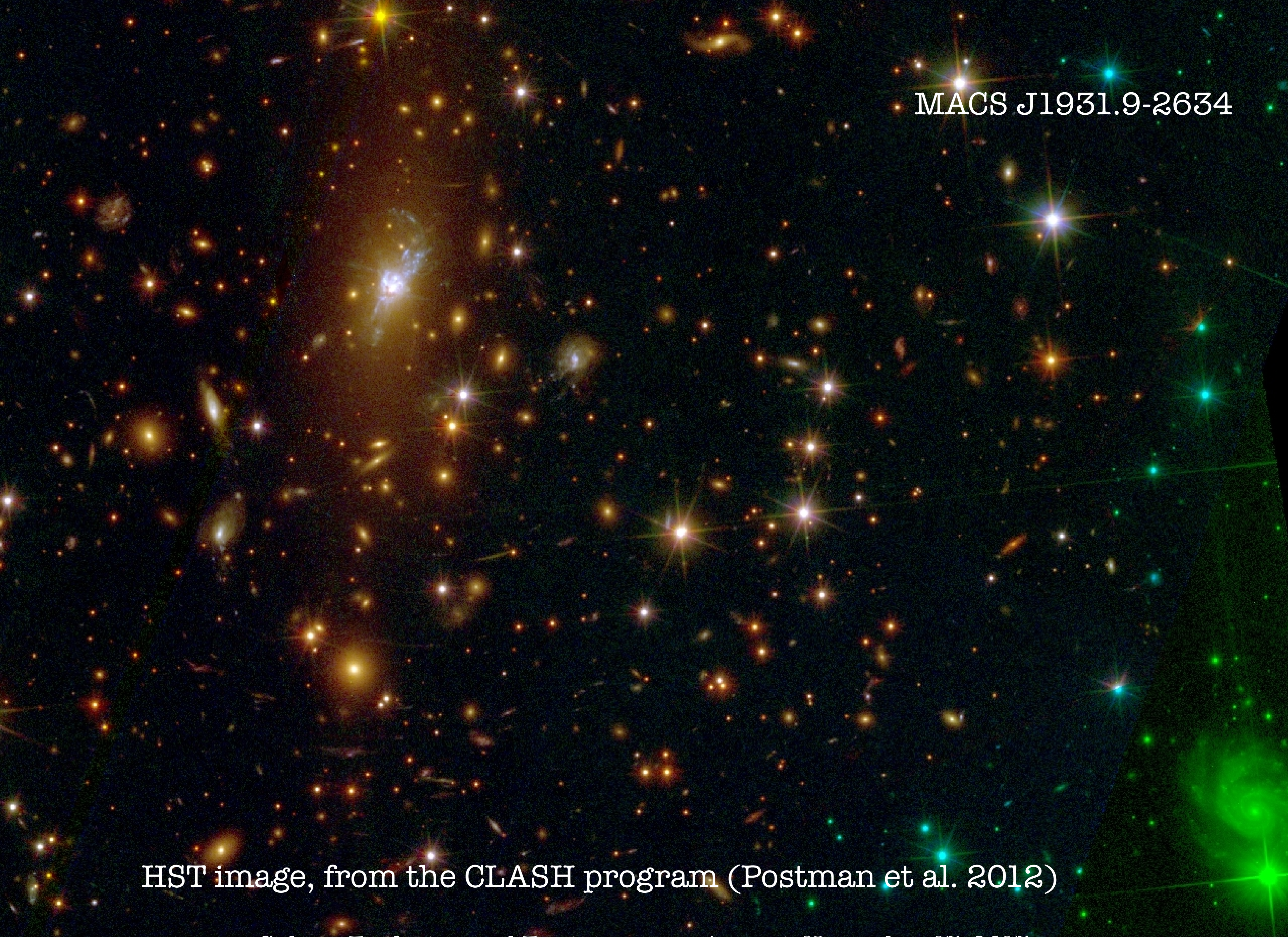
MACS J1931.9-2634
HST image, from the CLASH program (Postman et al. 2012)

Star formation in BCG across cosmic epochs

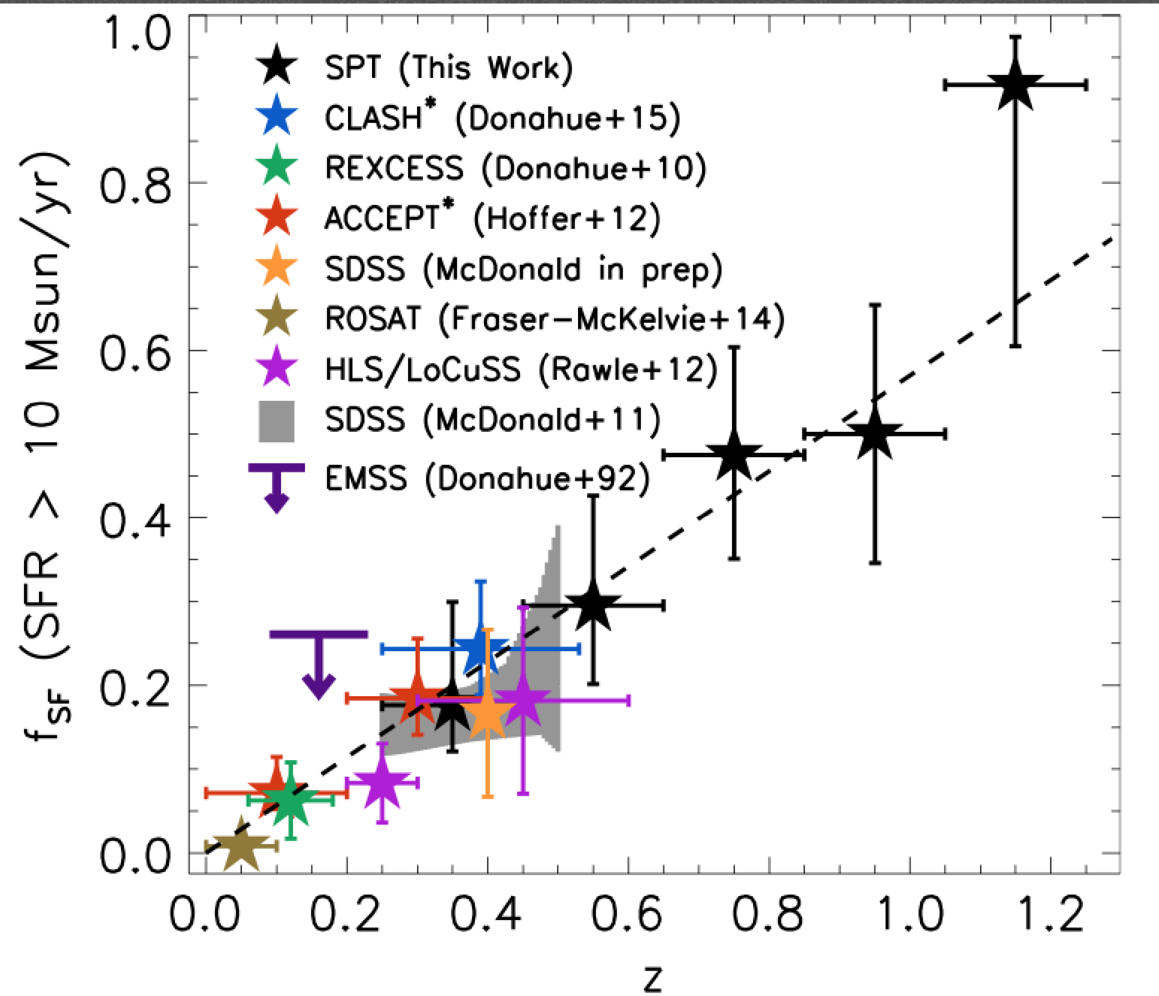

Figure 4. Fraction of BCGs with SFR > 10 $M_\odot$ yr^{-1} (f_{SF}) as a function of redshift. Black points show data from this work in four different redshift bins, while colored points show data from previous works over $0 < z < 0.6$

Mc Donald et al. 2016
increasing fraction of SF BCG
mostly associated to merger at z>1, and to cooling cores at z<1.
SF in BCG decreases with Time slower wrt the field

A direct link between the cool core and the SFR in the BCG

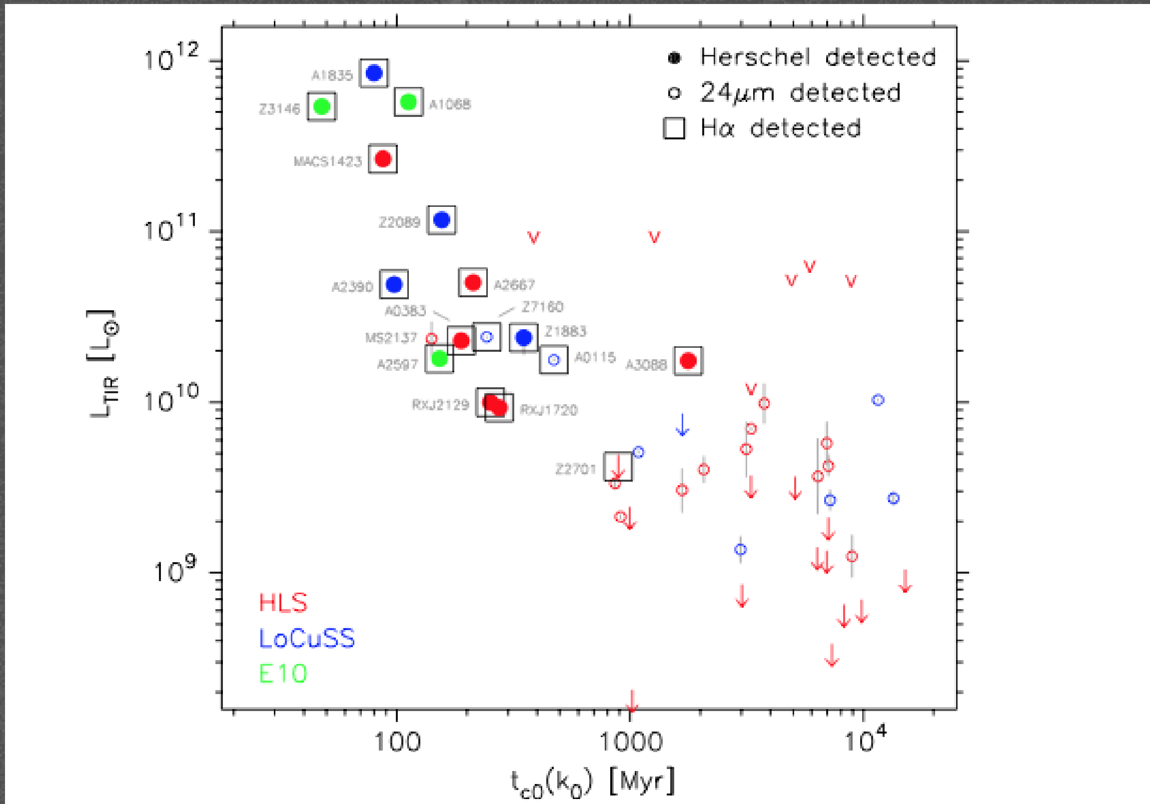

Mass deposition rate ~ 1/10 of that predicted by the isobaric CF model

SFR in the BCG ~= Residual cooling flow ~ 1/10 isobaric CF prediction

Rawle et al. 2012
Mittal et al. 2015

Simple scheme: the starburst is due to the immediate consumption of the cold gas flowing (or precipitating) from the ICM in the cool core

SFR larger than isobaric mass deposition rate allowed by the X-ray spectrum in MACSJ1931

$$\frac{dL}{dT} \propto \frac{5}{2}\frac{\dot{M}\,k}{\mu\, m_P}$$

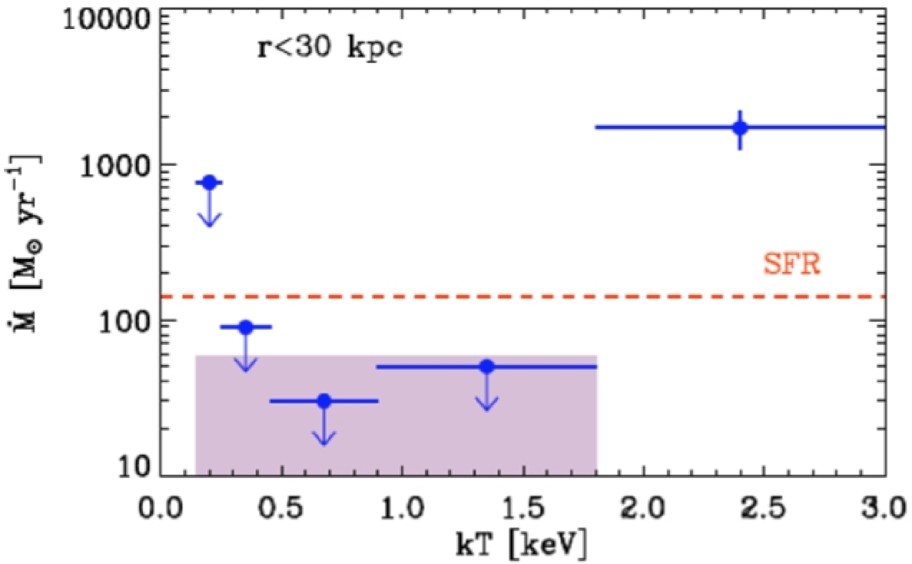

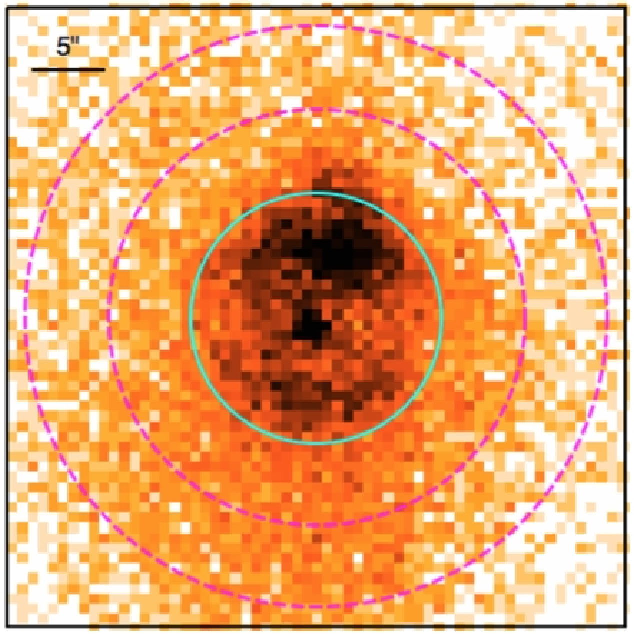

Santos et al. (2016)

Limits on the isobaric cooling rate in cool core clusters

Name	z	SFR $M_\odot$ yr^{-1}	SFR Orig.[a]	SFR Ref.[b]	$M_{\rm mol}$[c] 10^{10} $M_\odot$	$M_{\rm mol}$ Ref.[d]
A1835	0.252	146	IR SED	Ra12	5.0	Mn14
RXC J1504.1	0.215	140	H_α	Og10	–	–
RX J1532.9+3021	0.345	110	70 μm	Ho12	12.5[e]	Ed01
A1068	0.139	99.3	IR SED	Ra12	3.7[f]	Sa03
ZW 3146	0.291	93.1	IR SED	Ra12	8.0[e]	Ed01
Z0348	0.254	32.6	IR SED	Ra12	–	–

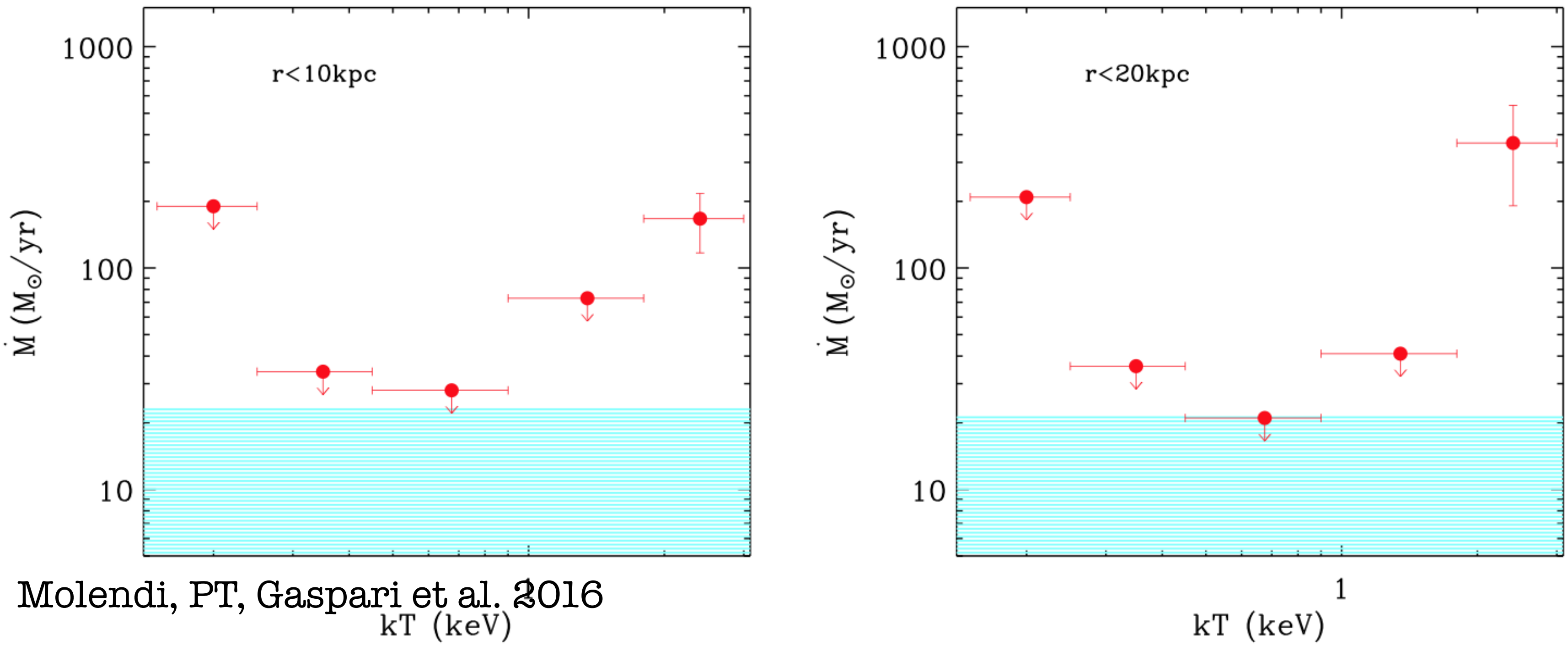

Molendi, PT, Gaspari et al. 2016

Current limits on isobaric cooling flows are lower than observed SFR. Way out: SF events naturally slower and non-isobaric cooling

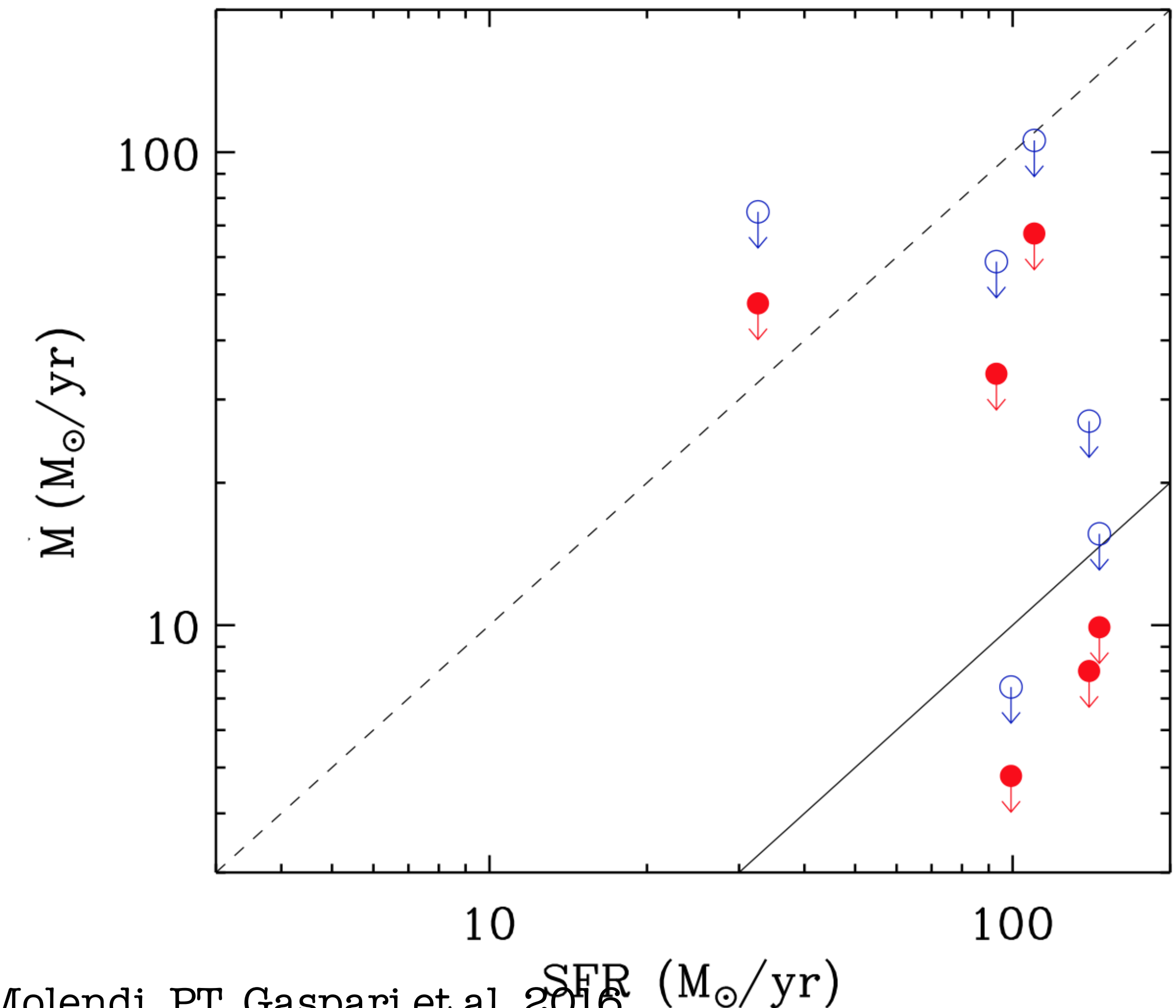

Molendi, PT, Gaspari et al. 2016

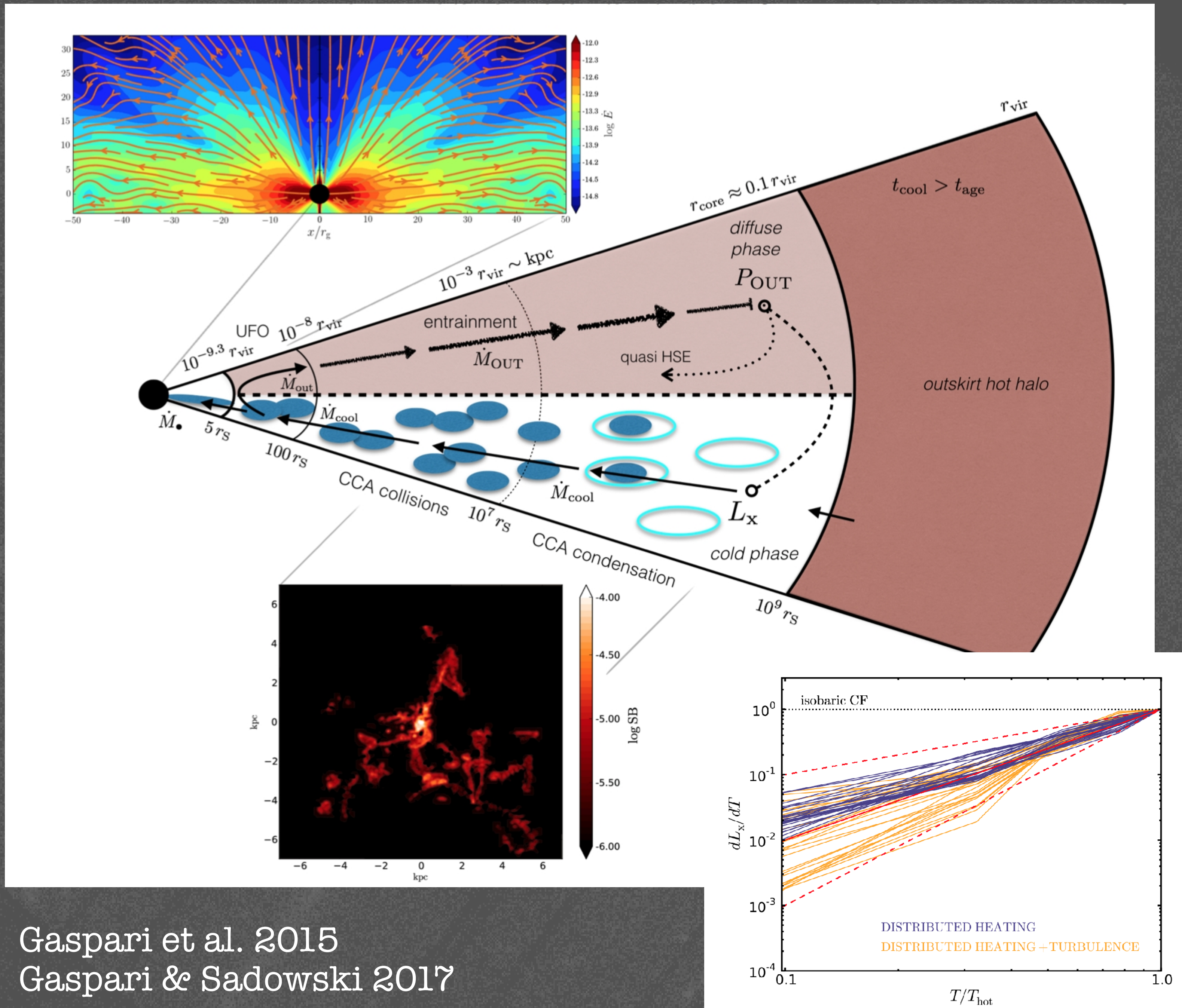

Gaspari et al. 2015
Gaspari & Sadowski 2017

Yu et al. 2017 arXiv:1707.05336

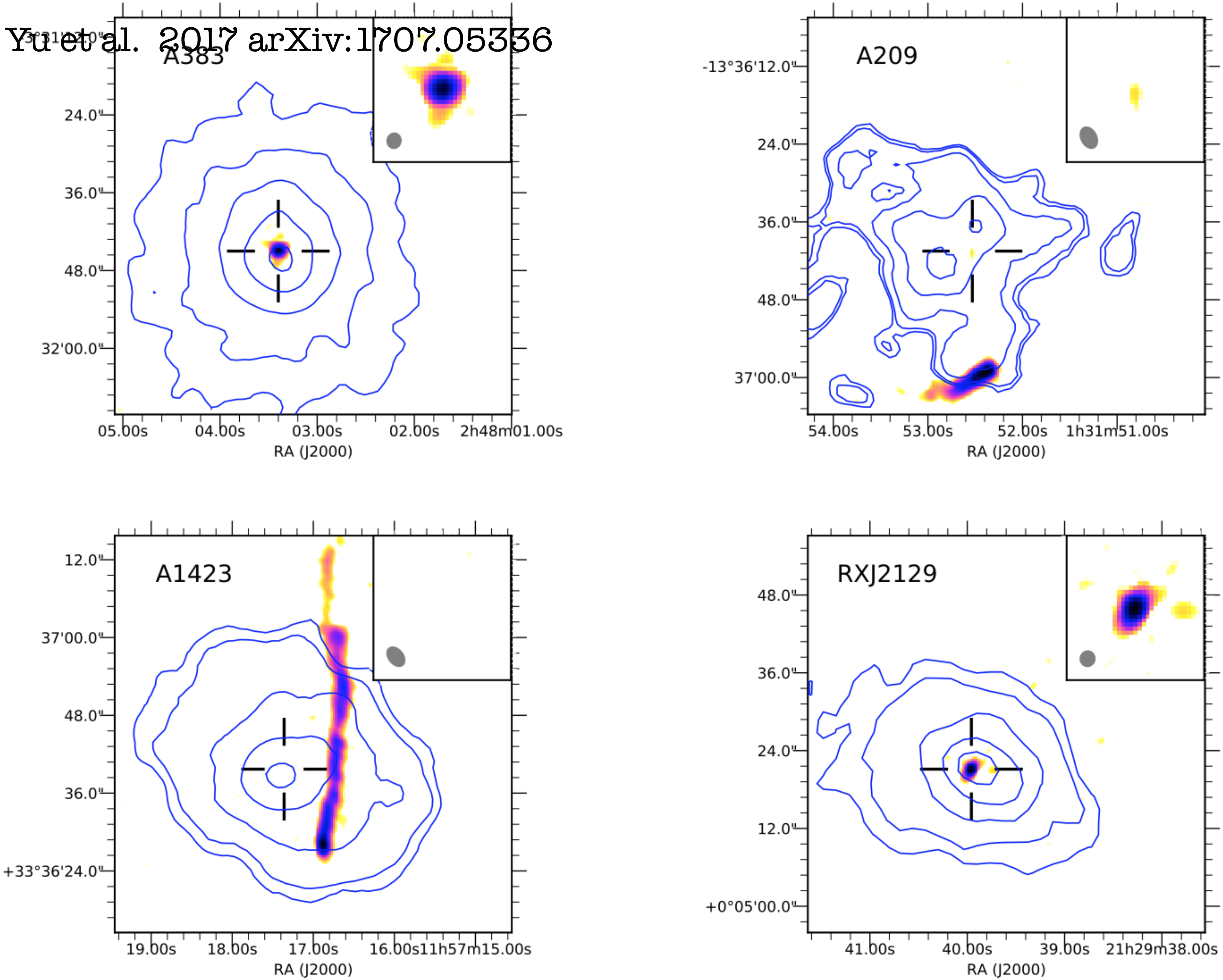

Yu et al. 2017 arXiv:1707.05336

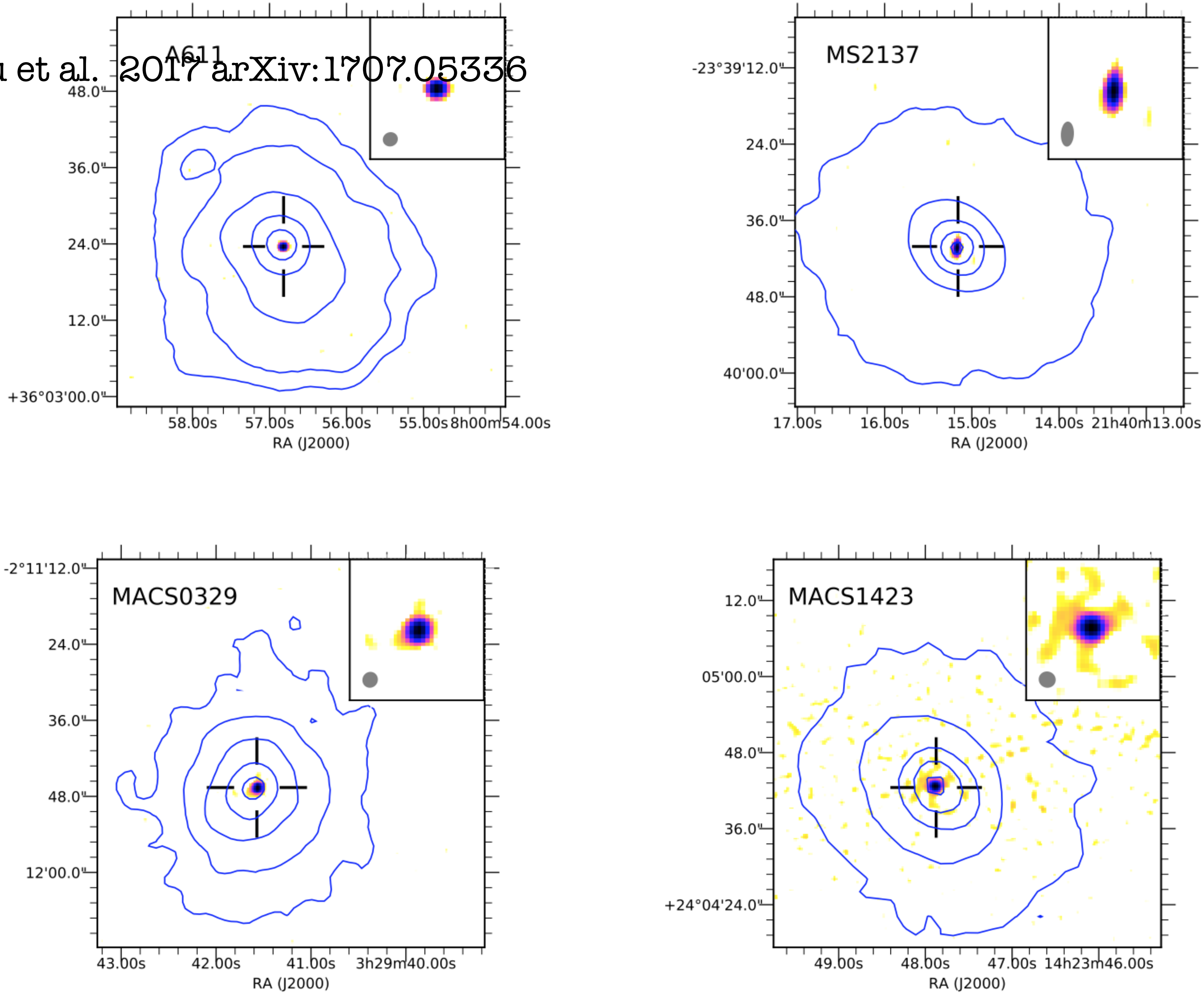

Yu et al. 2017 arXiv:1707.05336

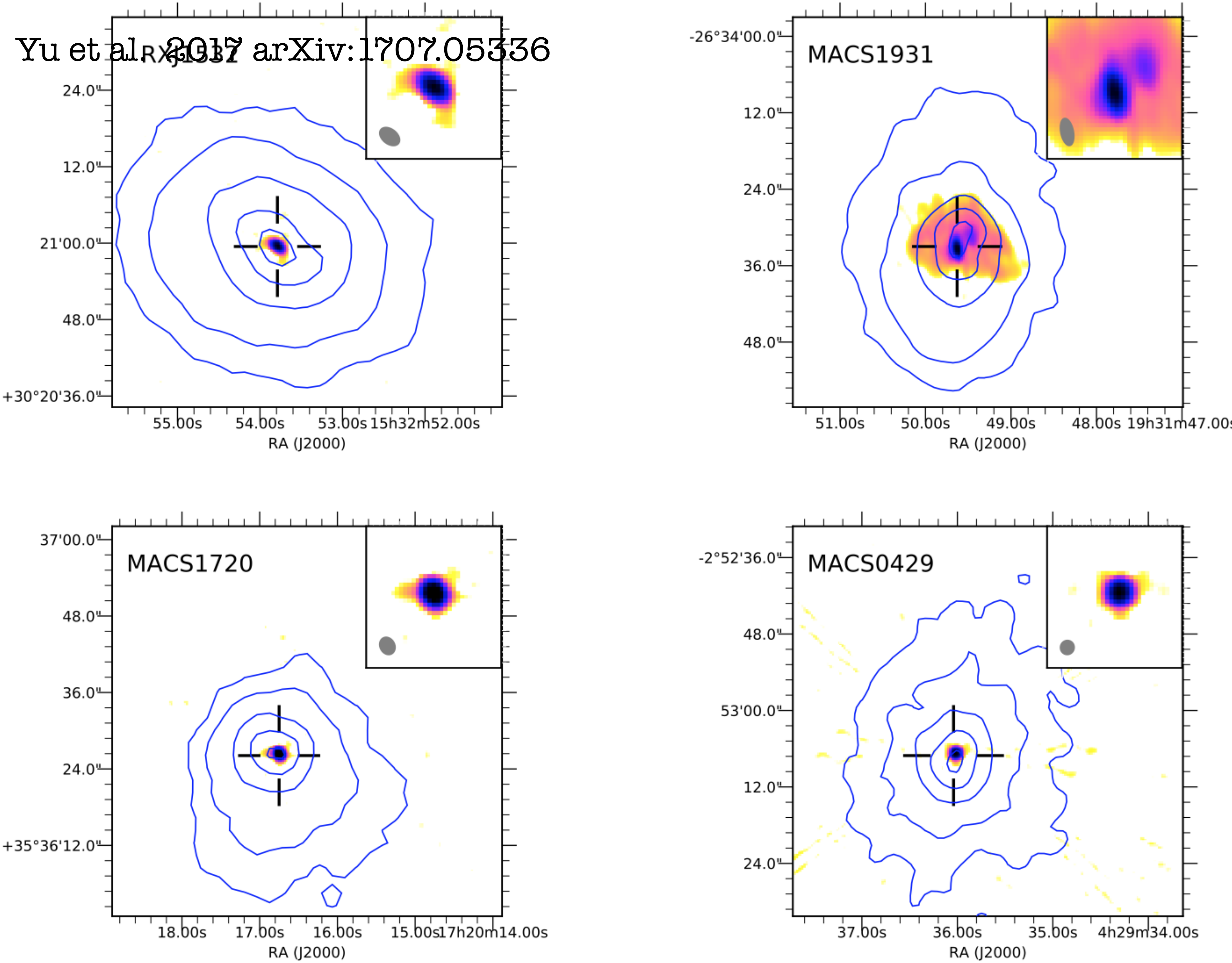

Yu et al. 2017 arXiv:1707.05336

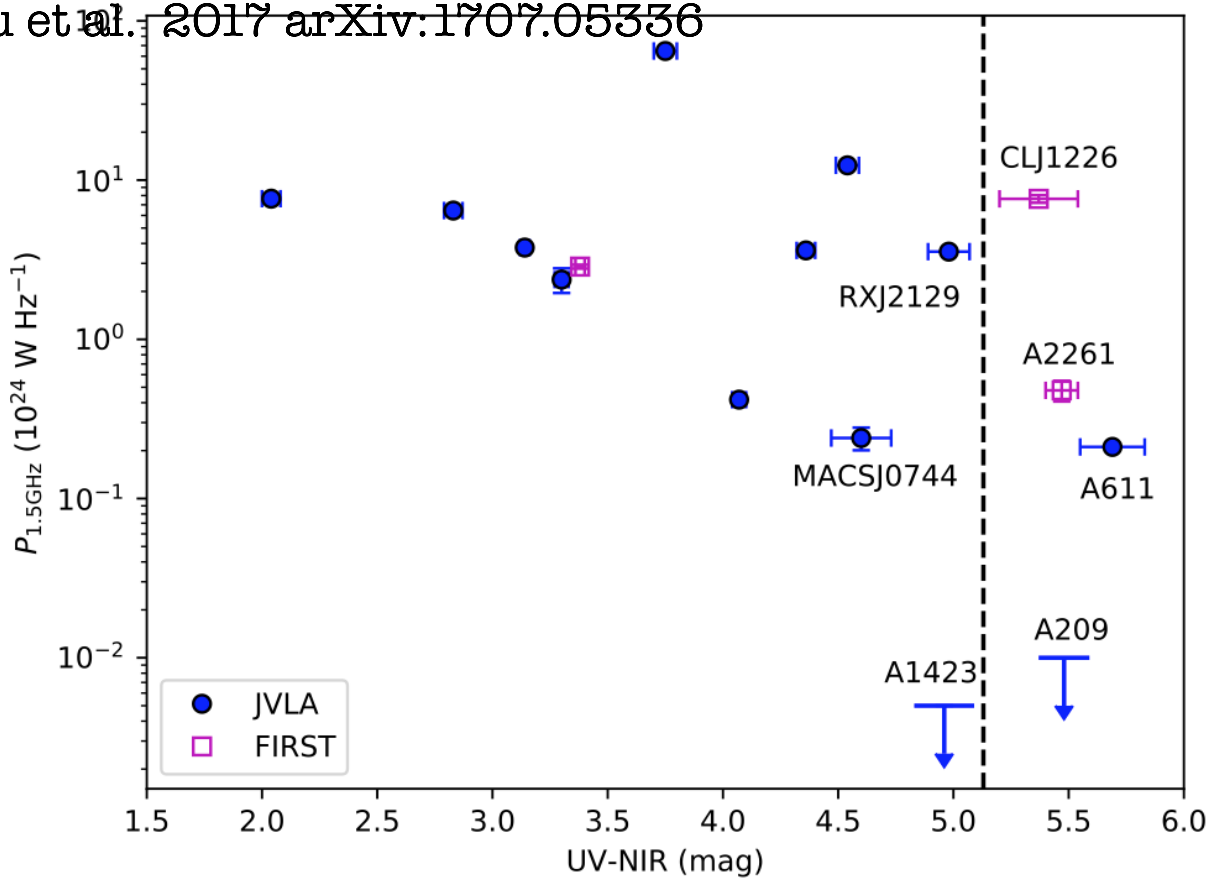

FIG. 7.— Radio power of BCGs measured in this work plotted vs the rest frame UV (280 nm) - NIR (1 μ) color of BCGs (from Donahue et al. 2015). The dashed mark the threshold $UV - NIR = 5.13$ which is the average color of quiescent BCGs in CLASH sample. **Solid circles correspond to the sources observed with JVLA in this work, while empty squares are obtained from FIRST.**

Yu et al. 2017

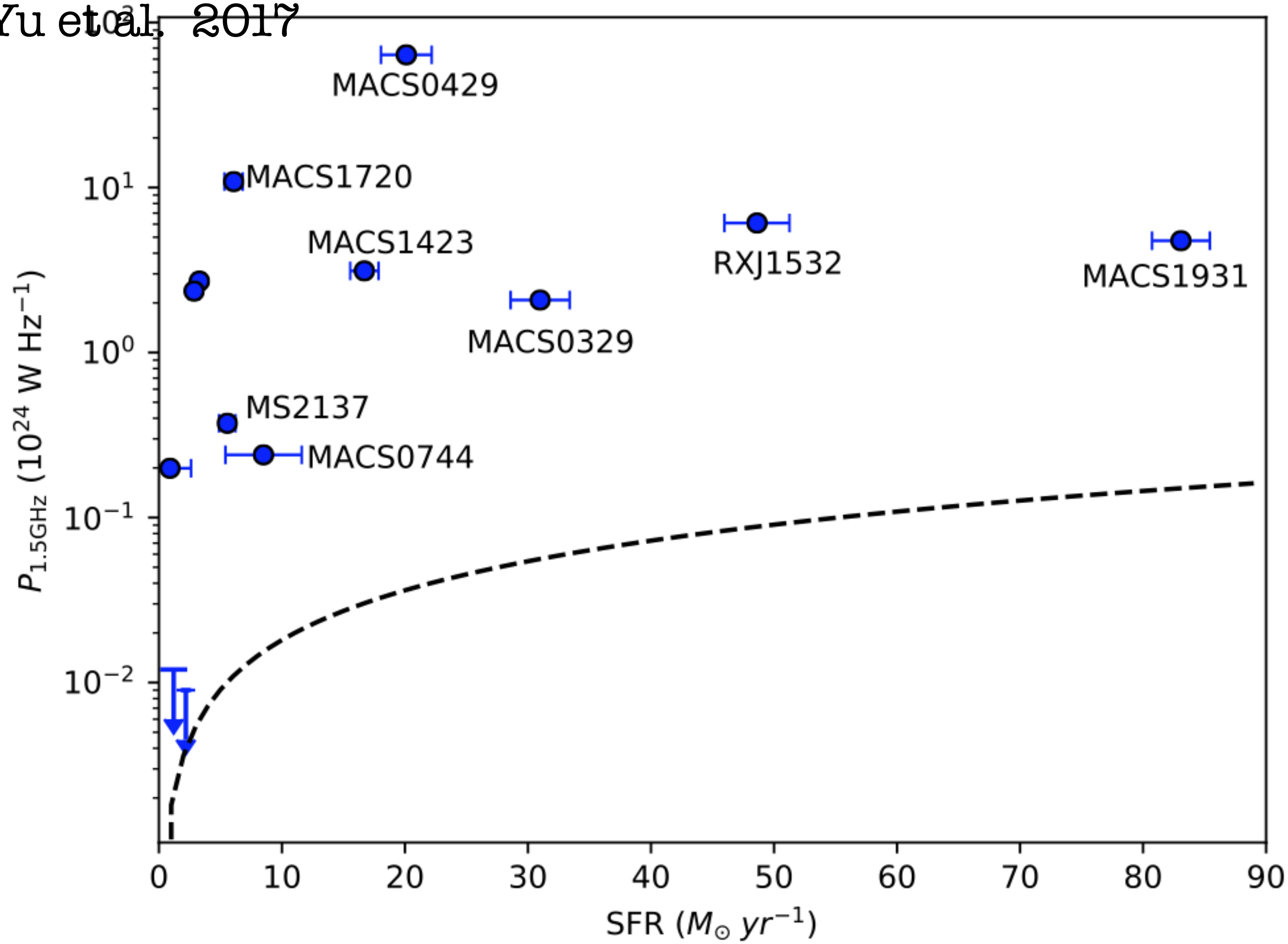

FIG. 10.— Radio luminosity vs star formation rate as measured from the excess UV luminosity, after Donahue et al. (2015). The dashed line shows the radio luminosity associated to star formation events derived by Bell (2003).

Yu et al. 2017 arXiv:1707.05336

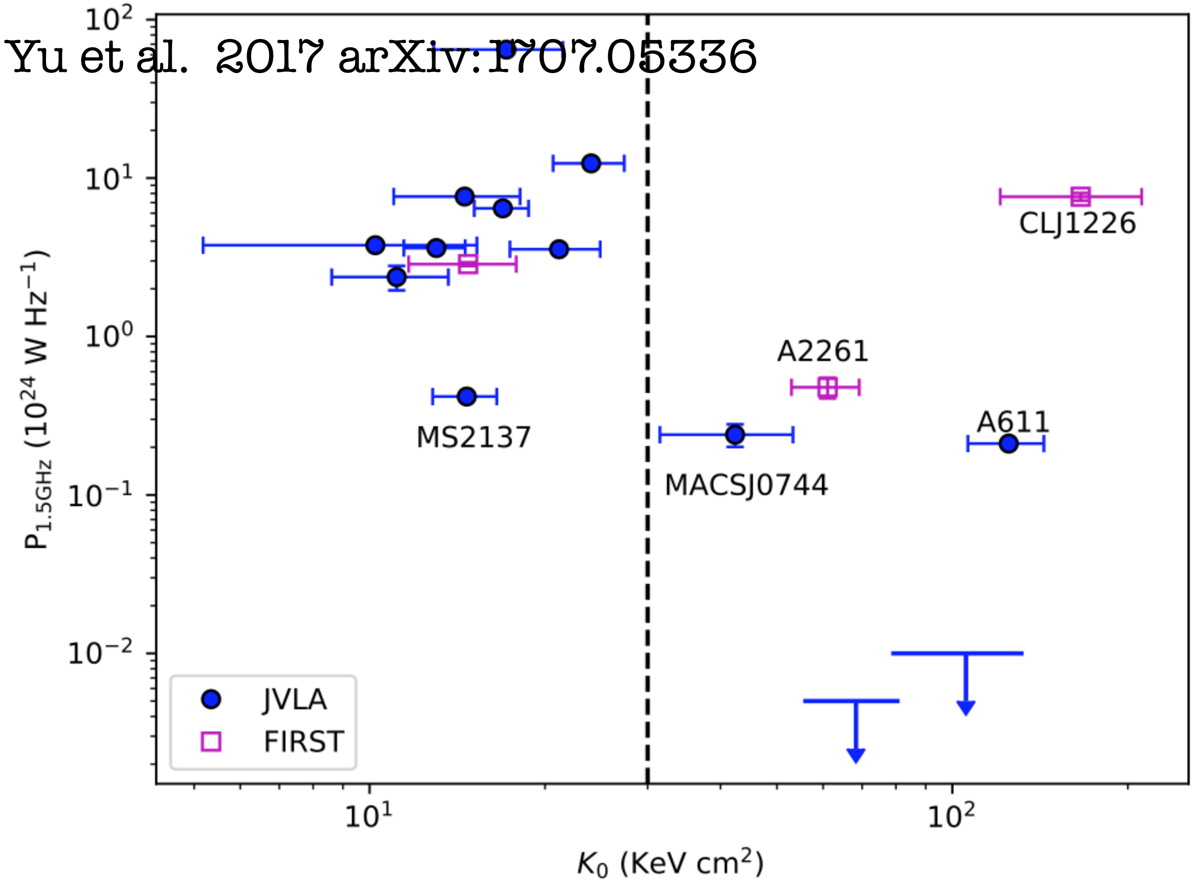

FIG. 6.— Nuclear radio power of BCG measured in this work versus the central X-ray gas entropy as estimated in ACCEPT (Cavagnolo et al. 2009). The dashed line corresponds to the threshold $K_0 = 30$ keV cm^2 as indicated by Cavagnolo et al. (2008) as the transition between clusters hosting BCGs with multi-phase gas, radio sources, and star formation, and clusters hosting quiescent BCGs. Solid circles correspond to the sources observed with JVLA in this work, while empty squares are obtained from FIRST.

Yu et al. 2017 arXiv:1707.05336

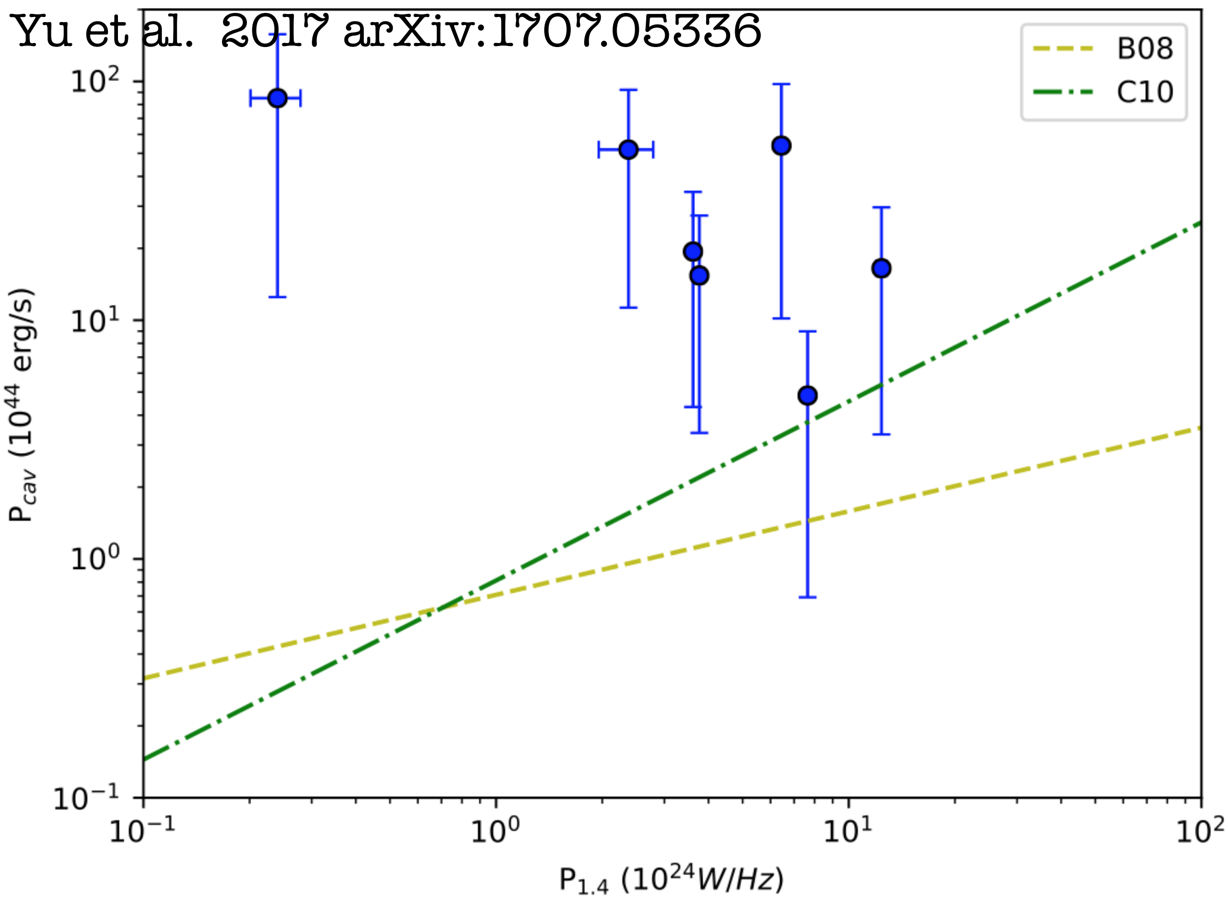

FIG. 9.— Upper panel: the total enthalpy as measured from the size of the cavities, taken from Shin et al. (2016), vs the radio power of the BCGs. Lower panel: the average mechanical power, computed dividing the enthalpy of each cavity by the buoyancy time, according to Bîrzan et al. (2004). The yellow dashed line represents the best-fit power law relation presented in Bîrzan et al. (2008), while the green dot-dashed line is the relation from Cavagnolo et al. (2010).

Conclusions

Searching for high-z (z>1.6-2) clusters and trace the formation phases of the BCG and the halo dynamics/virialization at the same time

Finding the gas cooling from the ICM via short-live isobaric cooling episodes or more complex process (like Chaotic Cold Accretion)

Follow recurrent star formation episodes (and metal production and diffusion) processes in BCG up to the highest z

Derive the duty cycle of the different modes of accretion (feeding) and of the associated nuclear activity responsible for the mechanical-mode feedback